IEEE Photonics Journal
An IEEE Photonics Society Publication

Open Access

Flexible ITO-Free Organic Solar Cells Based on MoO_3/Ag Anodes

Volume 7, Number 1, February 2015

Zhizhe Wang
Chunfu Zhang, Member, IEEE
Dazheng Chen
Shi Tang
Jincheng Zhang
Ying Wang
Genquan Han
Shengrui Xu
Yue Hao, Senior Member, IEEE

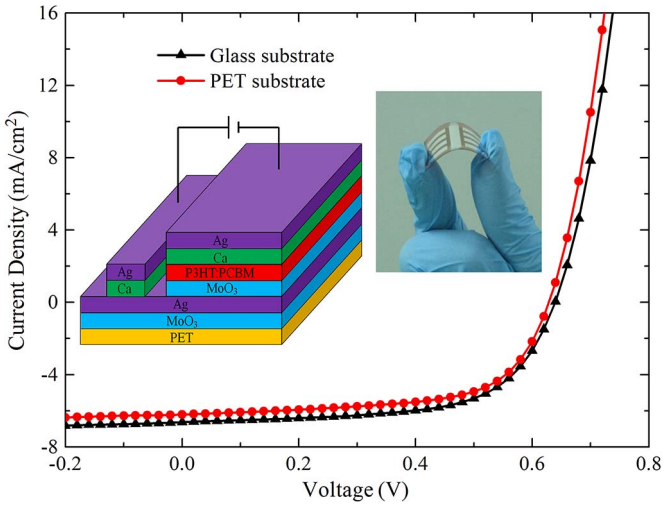

DOI: 10.1109/JPHOT.2015.2396906

IEEE photonics SOCIETY

IEEE

Flexible ITO-Free Organic Solar Cells Based on MoO_3/Ag Anodes

Zhizhe Wang, Chunfu Zhang, *Member, IEEE*, Dazheng Chen, Shi Tang, Jincheng Zhang, Ying Wang, Genquan Han, Shengrui Xu, and Yue Hao, *Senior Member, IEEE*

State Key Discipline Laboratory of Wide Band Gap Semiconductor Technology, School Of Microelectronics, Xidian University, Xi'an 710071, China

DOI: 10.1109/JPHOT.2015.2396906

Manuscript received December 27, 2014; revised January 19, 2015; accepted January 21, 2015. Date of publication January 26, 2015; date of current version February 18, 2015. This work was supported in part by the National Natural Science Foundation of China under Grant 61334002 and Grant 61106063, and the Fundamental Research Funds for the Central Universities under Grant JB141106.
Corresponding authors: C. Zhang and Y. Hao (e-mail: cfzhang@xidian.edu.cn; yhao@xidian.edu.cn).

Abstract: Flexible organic solar cells (OSCs) using our proposed MoO_3 (2 nm)/Ag (9 nm) anode are fabricated on poly(ethylene terephthalate) (PET) substrates with poly(3-hexylthiophene) (P3HT) and [6,6]-phenyl-C61 -butyric acid methyl ester (PCBM) films as the active layer. Power conversion efficiency (PCE) of 2.50% is achieved for such flexible indium tin oxide (ITO)-free OSCs under 1 sun AM 1.5G simulated illumination, which is comparable with that of the same devices fabricated on glass substrates (PCE of 2.71%) or that of ITO-based reference OSCs on glass (PCE of 2.85%). Meanwhile, such flexible ITO-free OSCs show good mechanical flexibility. A 10% degradation in PCE is observed after 500 inner bending cycles with a bending radius of 1.5 cm, whereas a 5% decrease in PCE is observed after 500 outer bending cycles. Furthermore, the flexibility of the structure PET/MoO_3/Ag/MoO_3 has been investigated. Its transparency almost remains constant, and its sheet resistance varies negligibly after 1000 cycles of inner or outer bending tests. It shows the huge potential of our flexible electrodes, and it may be instructive for further research on flexible electrodes.

Index Terms: Flexible, ITO-free, MoO_3/Ag electrodes, organic solar cells.

1. Introduction

Organic solar cells (OSCs) have recently attracted tremendous academic and industrial attention with the huge potential of supplementing other forms of renewable energy resources in quenching the world's thirst for increasing energy supply [1]. Research over the past decade has shown that OSCs are no longer considered as only a interesting area of academic research but are realistic alternative to established photovoltaic technologies [2], [3]. As we all know, a major advantage of OSCs is the variety of polymer and composites that can be employed as the active layer; thus, this offers many avenues in further improving the device performance [4]. Moreover, compared with their inorganic counterparts, OSCs have many advantages such as low cost [5], the internal quantum efficiency approaching 100% [6], light weight, low-temperature solution processing [7], and, of course, their considerable flexibility.

Indium tin oxide (ITO) sputtered on glass has been the commonly-used transparent electrode in OSCs since it has the best combination of high optical transparency and low sheet

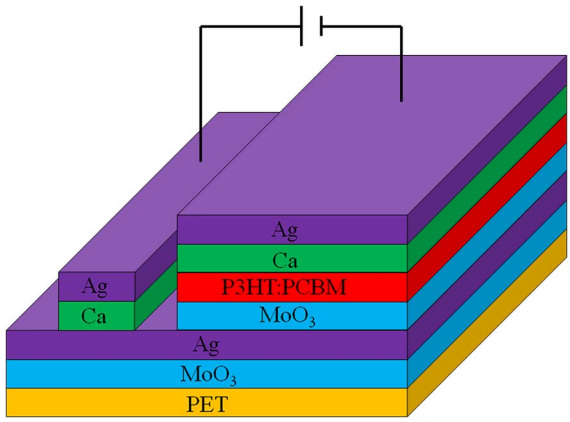

Fig. 1. Device geometry of ITO-free OSCs fabricated on PET substrates.

resistance. However, the flexible electrode with low cost is the prerequisite for cheap roll-to-roll mass fabrication of OSCs, for which ITO is unsuitable. For example, ITO is brittle due to its ceramic structure, which can induce defects when it is too much flexed [8]–[11]. Moreover, high temperature process conditions (usually sputter) in the fabrication of ITO electrode make it incompatible with flexible substrates [12]. Meanwhile the scarce indium source and a heavy demand from flat-panel display industry lead to high cost for ITO electrode [13]. Thus, ITO electrodes have already become a bottleneck for commercialization of OSCs. More and more works are dedicated to alternative transparent conductive electrodes. Besides indium-free transparent conducting oxides (such as Ga-doped ZnO (GZO) and Al-doped ZnO (AZO)) [14]–[16], poly(3,4-ethylenedioxythiophene): poly-(styrenesulfonate) (PEDOT:PSS) [17], [18], Ag nanowires [12], [19], graphene [13] and carbon nanotubes [20] are proposed as the replacement of ITO electrode. However, although GZO or AZO has a lower cost than ITO, high temperature sputter process in the fabrication of these electrodes still has the detrimental effect on flexible substrates. Although the PEDOT:PSS electrode can be fabricated by simple solution method, the conductivity of this electrode is still not good enough [1], [21]. The surface of Ag nanowire, graphene and carbon nanotube electrodes are usually rough, limiting charge injection into or extraction from the active layer [12], [13], [22]. In addition, complex film processing of these electrodes also makes them unsuitable for the fabrication of large-scale OSCs [12], [13], [22].

On the contrary, a smooth metal thin film (for example Ag) can be deposited on flexible substrates by simple thermal evaporation, without harm to the plastic substrates. Moreover, the ductile nature and high conductivity of metal thin film electrodes make them suitable for roll-to-roll mass production of OSCs [22]. Thus, increasingly more attention is focused on this topic. Various metal thin film electrodes (such as Au [23], Ag [3], Cu [24], Cu/Ni [25], $MoO_3/Au/MoO_3$ [22], and so on) are proposed and employed as the alternative of ITO electrode.

In our previous work [26], [27], $(MoO_3)/Ag$ electrodes have been investigated in the view of how to reduce the metal percolation threshold. After the study of the electrical, optical and morphological properties of $(MoO_3)/Ag$ electrodes deposited onto glass substrates, the optimal MoO_3 (2 nm)/Ag (9 nm) electrode is obtained due to its good properties in optical transparency and electrical conductivity. In this paper, this investigation has been extended to the realization of transparent conductive electrodes onto flexible substrates. Based on this MoO_3 (2 nm)/Ag (9 nm) anode, ITO-free OSCs are fabricated on flexible poly(ethylene terephthalate) (PET) substrates, with poly (3-hexylthiophene) (P3HT) and [6,6]-phenyl-C61 -butyric acid methyl ester (PCBM) films as the active layer. The devices are composed as follows: $PET/MoO_3/Ag/MoO_3$/P3HT:PCBM/Ca/Ag (see Fig. 1). Here, the MoO_3 layer adjacent to the active layer works as the hole transport layer with high work function. A power conversion efficiency (PCE) of 2.50% is achieved for such flexible OSC under 1 sun AM 1.5G simulated illumination, comparable to that of the same device on the rigid glass substrate (PCE of 2.71%). Meanwhile, our ITO-free OSCs based on PET substrates

show good mechanical flexibility. A 10% degradation in PCE is observed after 500 inner bending cycles with a bending radius of 1.5 cm, while a 5% decrease in PCE is observed after 500 outer bending cycles. Further, the flexibility of the structure PET/MoO_3/Ag/MoO_3 has been investigated. Its transparency almost keeps constant, and its sheet resistance varies negligible after 1000 bending cycles with a bending radius of 1.5 cm, regardless of matter inner or outer bending tests. This excellent flexibility of our MoO_3 (2 nm)/Ag (9 nm) electrode shows its huge potential for the application in roll-to-roll mass fabrication of OSCs. It is instructive for further research of flexible electrodes and OSCs.

2. Experimental Section

2.1. Material and Substrate Preparation

P3HT was purchased from Rieke Metals Inc., PCBM was purchased from Nano-C Inc., and 1,2-dichlorobenzene and MoO_3 were provided from Aldrich Inc. All the materials were used without any further purification. P3HT and PCBM were dissolved in 1,2-dichlorobenzene with a concentration of 20 mg/mL, respectively. They were mixed in a weight ratio of 1 : 0.8 and stirred at room temperature for 2 h before use. 188 μm thick PET substrates were cleaned sequentially with detergent (Decon 90, UK), deionized water, acetone, and ethanol in an ultrasonic bath for about 5 min.

2.2. Electrode Deposition and Characterization

Cleaned PET substrates were dried with a nitrogen (N_2) flow and then directly transferred into a custom-made multichamber ultrahigh vacuum evaporation system without further planarization. The MoO_3/Ag electrodes were deposited on PET by thermal evaporation at a vacuum pressure $< 5 \times 10^{-4}$ Pa, with a evaporation rate of 0.02 and 0.1 nm/s for MoO_3 and Ag, respectively. The substrates during deposition were at room temperature. The thicknesses and evaporation rates were estimated in situ with a calibrated quartz crystal monitor.

The spectral transmission was recorded by using an UV-VIS-NIR spectrophotometer (Lambda 950, Perkin Elmer). Since transmission was measured relative to air, the reflection of the substrate was included. The sheet resistances of the samples were measured by using a four-point probe setup.

2.3. Device Fabrication and Measurement

After the electrode deposition, a 10 nm thick MoO_3 layer was first thermally evaporated onto the substrates as the anode buffer layer. Then, P3HT:PCBM solution was spin-coated onto the samples at 1000 rpm for 60 s in a N_2 glove box attached to the vacuum system, followed by annealed at 135 °C for 10 min. Finally, 10 nm thick Ca and 70 nm thick Ag were further deposited on top of the active layer as the cathode through a metal shadow mask to finish the flexible OSCs, resulting in an active solar cell area of 12.5 mm^2. Reference OSCs were fabricated on glass substrates through nearly the same procedure except that they were annealed at 150 °C. The current density-voltage $(J-V)$ characteristics were measured with a source measurement unit 2400 SMU (Keithley, USA) and simulated AM 1.5G sun light (San-Ei Electric) in air with no device encapsulation. The illumination intensity was kept at 100 mW/cm^2 through using a Si standard solar cell calibrated by the National Renewable Energy Laboratory (NREL).

3. Results and Discussion

The illuminated $J-V$ characteristics of ITO-free OSCs fabricated on PET or glass substrates are depicted in Fig. 2. For comparison, the corresponding photovoltaic parameters have been demonstrated in the inset of Fig. 2. Meanwhile, a photograph of a bent flexible ITO-free device has also been shown as the inset of Fig. 2. As shown in Fig. 2, a PCE of 2.71% is achieved for the devices fabricated on glass substrates, with a open-circuit voltage (V_{OC}) of 0.64 V, a short-circuit current density (J_{SC}) of 6.63 mA/cm^2 and a FF of 64%, comparable to that of ITO-based

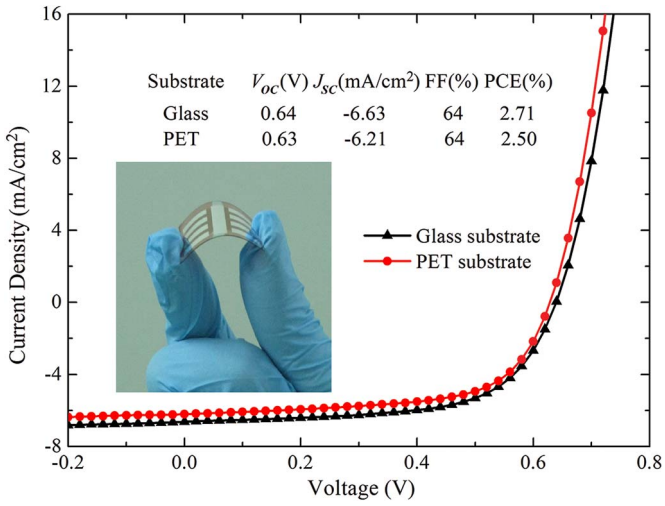

Fig. 2. $J-V$ characteristics for ITO-free OSCs fabricated on PET or glass substrates under 1 sun AM 1.5G simulated illumination. For comparison, the corresponding photovoltaic parameters have been shown here as an inset. Meanwhile, a photograph of a bent flexible ITO-free device is also shown the inset.

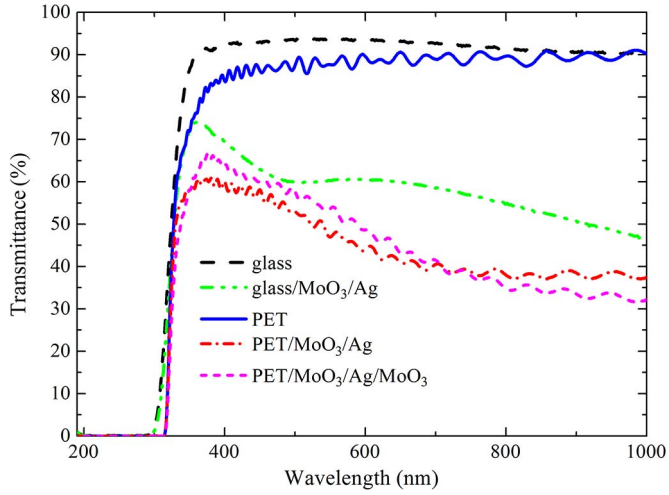

Fig. 3. Wavelength-dependent transmittance spectra of PET, glass, glass/MoO_3 (2 nm)/Ag (9 nm), PET/MoO_3 (2 nm)/Ag (9 nm), and PET/MoO_3 (2 nm)/Ag (9 nm)/MoO_3 (10 nm).

reference OSCs (PCE of 2.85%), and the flexible ITO-free OSCs fabricated on PET substrates show similar performance as the devices on the rigid glass substrates, with a V_{OC} of 0.63 V, a J_{SC} of 6.21 mA/cm^2, a FF of 64% and a PCE of 2.50%. Compared with the performance of ITO-free OSCs fabricated on glass substrates, V_{OC} and FF of the flexible OSCs are nearly identical while J_{SC} is slightly smaller. To study the effect of different substrates on the performance of OSCs, the electrode-only samples of PET/MoO_3/Ag and glass/MoO_3/Ag are fabricated through the same procedure as the device production and used for the physical characterization.

The wavelength-dependent transmittance spectra of the above electrode-only samples are shown in Fig. 3. For comparison, the transmittance spectra of PET, glass and PET/MoO_3/Ag/MoO_3 are also depicted in Fig. 3. A good transparency is achieved for MoO_3 (2 nm)/Ag (9 nm) electrode fabricated on glass, with a maximum of 74% at 361 nm. In particular, in the visible region, the transparency of the electrode between 56% and 70% is achieved, showing the potential of this electrode. When this electrode is fabricated on flexible substrates, its transparency has

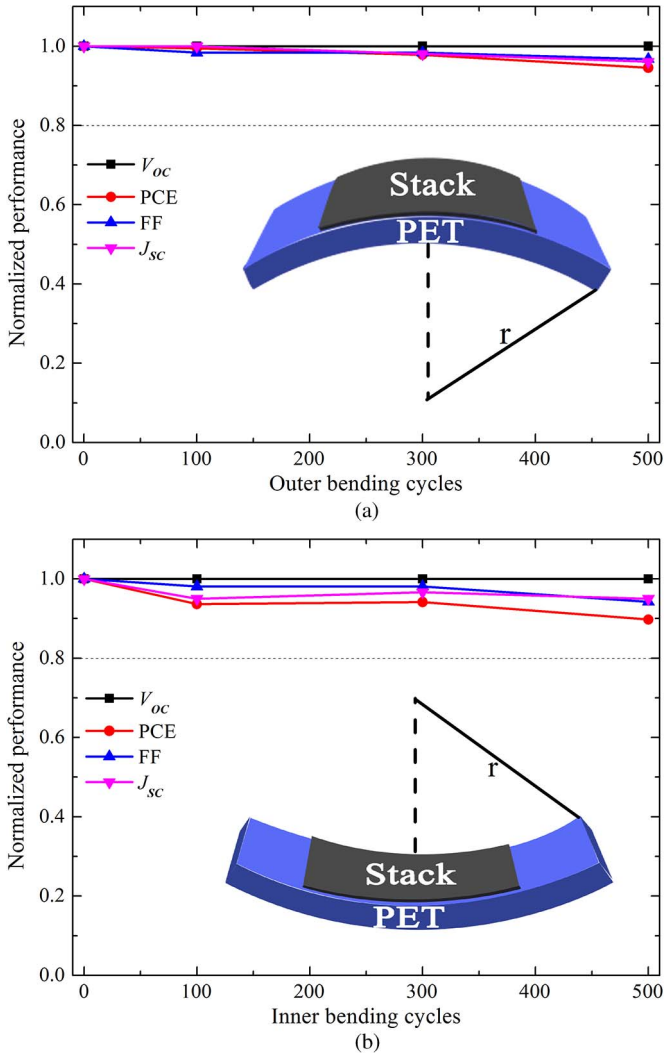

Fig. 4. Normalized photovoltaic performance parameters of flexible ITO-free OSCs as a function of the number of (a) outer or (b) inner bending cycles. (a) (Inset) Schematic drawing of outer bending configuration. *r* in the inset represents the bending radius. (b) (Inset) Schematic drawing of inner bending configuration.

been decreased to some extent in the nearly entire spectral range discussed, with a maximum of 61% at 381 nm, as shown in Fig. 3. Lower transparency of the flexible electrode leads to a slightly smaller JSC of 6.21 mA/cm^2 and a comparatively lower PCE of 2.50%, compared with that of ITO-free OSCs fabricated on glass substrates (J_{SC} of 6.63 mA/cm^2 and PCE of 2.71%). Obviously, the difference in the transparency of two electrodes originates from different substrates. As we all know, the surface morphology and structure of thermal evaporated metal films depend on metal type, substrate, temperature or surfactants [28]–[31]. Thus, different substrates (PET or glass) can leads to different surface morphology and structure of Ag thin film electrodes. This may result in the difference in transparency of two electrodes. Meanwhile, as shown in Fig. 3, the transparency of the glass substrate is better than that of the PET substrate. Thus, both factors above leads to lower transparency of the flexible ITO-free electrode, compared with that of the same electrode fabricated on glass substrates. Moreover, interestingly, it can be observed from Fig. 3 that the transparency of the stack has been improved when the MoO_3 buffer layer is deposited onto the flexible electrode. Due to the optical interference effect, compared with that of PET/MoO_3/Ag electrode, the transparency of the stack PET/MoO_3/Ag/MoO_3 in the

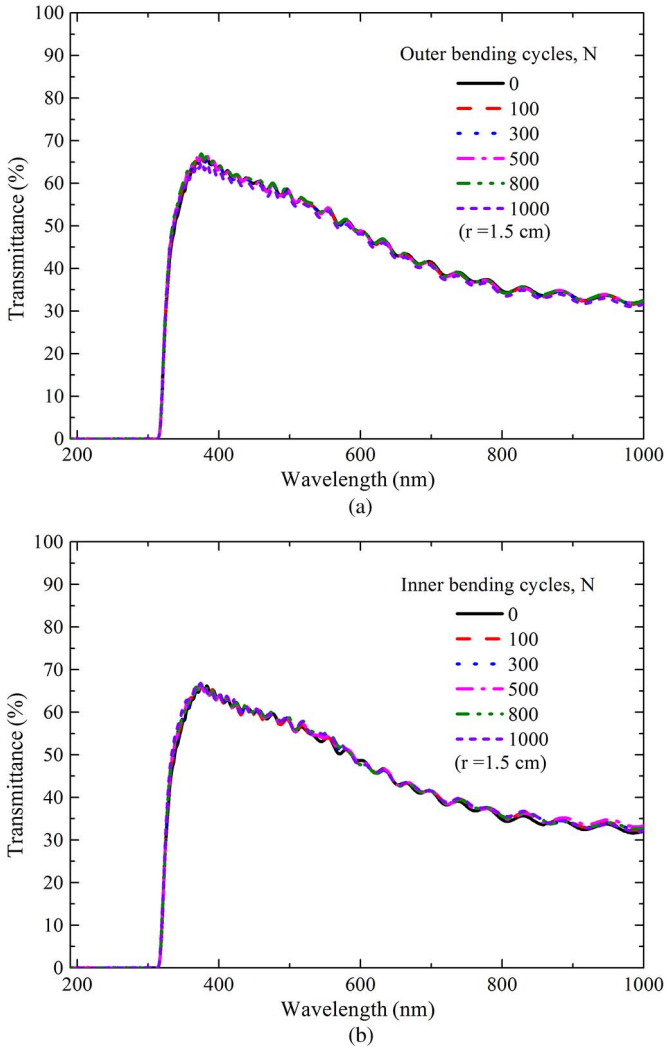

Fig. 5. Transparency of the stack PET/MoO_3/Ag/MoO_3 as a function of the number of (a) outer or (b) inner bending cycles.

spectral range between 350 and 700 nm has been increased with a maximum of 67% at 380 nm, while its transparency in the region over 700 nm has been decreased correspondingly. Since the photo-active materials are most efficient in the visible spectral range, the performance of the flexible ITO-free OSCs may be further enhanced by improving the transparency of the stack with the optimized MoO_3 buffer layer thickness. It will be discussed in our future work.

In order to check and quantitatively evaluate the flexibility of our ITO-free OSCs fabricated on PET substrates, the device performance has been measured after multiple cycles of outer or inner bending tests with a bending radius of 1.5 cm. Normalized photovoltaic performance parameters as a function of the number of outer or inner bending cycles are illustrated in Fig. 4(a) and (b), respectively. Schematic drawings of outer and inner bending configurations are also shown as the inset of Fig. 4(a) and (b), respectively. As shown in the inset of Fig. 4(a), for outer bending tests, the sample is bent with the stack (the electrode or the device) facing upward. However, for inner bending tests, the sample is bent in the opposite direction [see the inset of Fig. 4(b)]. It can be observed from Fig. 4(a) and (b) that V_{OC} of the device remains constant, even after 500 outer or inner bending cycles. Although after 500 outer bending cycles, J_{SC} and FF of flexible ITO-free OSCs decrease by 4% and 3%, respectively, resulting in a 5% decrease in PCE. The degradation of the device performance seems slightly faster for inner bending tests. After

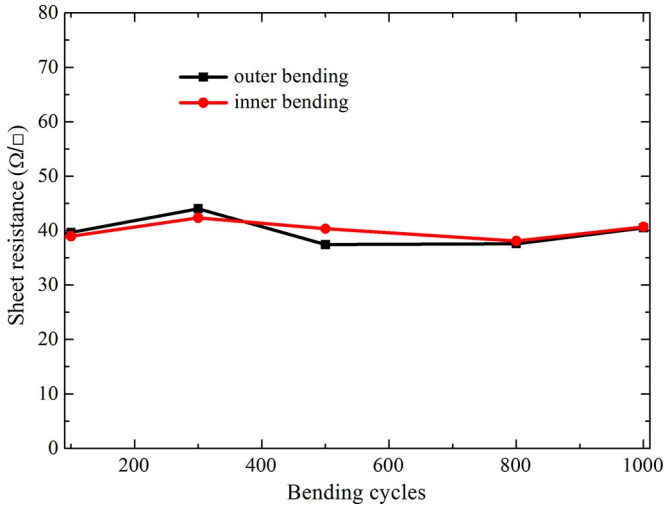

Fig. 6. Sheet resistance of the stack PET/MoO_3/Ag/MoO_3 as a function of the number of outer or inner bending cycles.

500 inner bending cycles, J_{SC} and FF decrease by 5% and 6%, respectively, resulting in a 10% degradation in PCE. The difference in the degradation of the OSC performance may be attributed to different stress the device bears for outer and inner bending tests.

For more in-depth study of the flexibility of our ITO-free electrodes fabricated on PET substrates, the transparency and sheet resistance of the structure PET/MoO_3/Ag/MoO_3 have been measured after outer or inner bending tests with a bending radius of 1.5 cm. The transparency of the stack PET/MoO_3/Ag/MoO_3 as a function of the number of outer or inner bending cycles is illustrated in Fig. 5(a) and (b), respectively. The sheet resistance of the stack as a function of outer or inner bending cycles is shown in Fig. 6. As shown in Fig. 5, the transparency of the stack almost keeps constant, even if after 1000 outer or inner bending cycles. Meanwhile, as illustrated in Fig. 6, after 1000 outer or inner bending cycles, the sheet resistance of the stack varies negligible.

Due to its advantage of high manufacturing speed, the printing technique has widely been used in roll-to-roll fabrication of large scale OSCs and tandem OSCs [32]–[34]. However, a dry process is essential in the fabrication of printed electrode structures, which limits the complete process speed [32]–[34]. Moreover, it also needs extra instruments, for example the oven, which increases the manufacture cost of printed electrodes. Flexible MoO_3/Ag electrode can be manufactured by a common vacuum roll-to-roll process, which has combined the advantages of vacuum deposition process and roll-to-roll process. Compared with printed flexible electrodes [32]–[34], although it takes more time in the deposition of MoO_3/Ag electrode, the fabrication of the electrode does not need a dry process. Thus the manufacturing speed of our flexible electrode may be comparable to those of printed flexible electrodes. The excellent performance of our flexible ITO-free electrode shows its huge potential for the application in roll-to-roll mass fabrication of OSCs. It is instructive for further research of flexible electrodes and OSCs.

4. Conclusion

In this paper, ITO-free OSCs are fabricated based on our proposed MoO_3 (2 nm)/Ag (9 nm) anode with P3HT:PCBM films as the active layer. A PCE of 2.71% is achieved for the devices fabricated on glass substrates under 1 sun AM 1.5G simulated illumination, comparable to that of ITO-based reference OSCs (PCE of 2.85%), and flexible ITO-free OSCs fabricated on PET substrates show a similar PCE of 2.50% as the devices on the rigid glass substrates. Meanwhile, such flexible ITO-free OSCs show good mechanical flexibility. A 10% degradation in PCE is observed after 500 inner bending cycles with a bending radius of 1.5 cm, while a 5% decrease in PCE is observed after 500 outer bending cycles. Further, the flexibility of the structure

PET/MoO_3/Ag/MoO_3 has been investigated. Its transparency almost keeps constant, and its sheet resistance varies negligible after 1000 bending cycles with a bending radius of 1.5 cm, regardless of the inner or outer bending tests. It shows the huge potential of our flexible electrodes and it may be instructive for further research of flexible electrodes.

References

[1] D. Angmo and F. C. Krebs, "Flexible ITO-free polymer solar cells," *J. Appl. Polymer Sci.*, vol. 129, pp. 1–14, Jul. 2013.
[2] S. Han, S. Lim, H. Kim, H. Cho, and S. Yoo, "Versatile multilayer transparent electrodes for ITO-free and flexible organic solar cells," *IEEE J. Sel. Topics Quantum Electron.*, vol. 16, no. 6, pp. 1656–1664, Nov./Dec. 2010.
[3] S. D. Yambem, K.-S. Liao, and S. A. Curran, "Flexible Ag electrode for use in organic photovoltaics," *Solar Energy Mater. Solar Cells*, vol. 95, no. 11, pp. 3060–3064, Nov. 2011.
[4] S. Curran, J. Talla, S. Dias, and J. Dewald, "Microconcentrator photovoltaic cell (the m-C cell): Modeling the optimum method of capturing light in an organic fiber based photovoltaic cell," *J. Appl. Phys.*, vol. 104, no. 6, Sep. 2008, Art. ID. 064305.
[5] N. S. Sariciftci, L. Smilowitz, A. J. Heeger, and F. Wudl, "Photoinduced electron transfer from a conducting polymer to buckminsterfullerene," *Science*, vol. 258, no. 5087, pp. 1474–1476, Nov. 1992.
[6] S. H. Park *et al.*, "Bulk heterojunction solar cells with internal quantum efficiency approaching 100%," *Nat. Photon.*, vol. 3, pp. 297–302, 2009.
[7] G. Li *et al.*, "High-efficiency solution processable polymer photovoltaic cells by self-organization of polymer blends," *Nat. Mater.*, vol. 4, pp. 864–868, 2005.
[8] J. Lewis, S. Grego, B. Chalamala, E. Vick, and D. Temple, "Highly flexible transparent electrodes for organic light-emitting diode-based displays," *Appl. Phys. Lett.*, vol. 85, no. 16, pp. 3450–3452, Oct. 2004.
[9] Y.-M. Chang, L. Wang, and W.-F. Su, "Polymer solar cells with poly(3,4-ethylenedioxythiophene) as transparent anode," *Org. Electron.*, vol. 9, pp. 968–973, Dec. 2008.
[10] C. D. Williams *et al.*, "Multiwalled carbon nanotube sheets as transparent electrodes in high brightness organic light-emitting diodes," *Appl. Phys. Lett.*, vol. 93, no. 18, Nov. 2008, Art. ID. 183506.
[11] M.-G. Kang, M.-S. Kim, and L. J. Guo, "Organic solar cells using nanoimprinted transparent metal electrodes," *Adv. Mater.*, vol. 20, no. 23, pp. 4408–4413, Dec. 2008.
[12] J.-Y. Lee, S. T. Connor, Y. Cui, and P. Peumans, "Solution-processed metal nanowire mesh transparent electrodes," *Nano Lett.*, vol. 8, no. 2, pp. 689–692, 2008.
[13] D. S. Hecht, L. Hu, and G. Irvin, "Emerging transparent electrodes based on thin films of carbon nanotubes, graphene, and metallic nanostructures," *Adv. Mater.*, vol. 23, pp. 1482–1513, Apr. 2011.
[14] H. Chen, A. Du Pasquier, G. Saraf, J. Zhong, and Y. Lu, "Dye-sensitized solar cells using ZnO nanotips and Ga-doped ZnO films," *Semicond. Sci. Technol.*, vol. 23, no. 4, Apr. 2008, Art. ID. 045004.
[15] H.-K. Park, J.-W. Kang, S.-I. Na, D.-Y. Kim, and H.-K. Kim, "Characteristics of indium-free GZO/Ag/GZO and AZO/Ag/AZO multilayer electrode grown by dual target DC sputtering at room temperature for low-cost organic photovoltaics," *Solar Energy Mater. Solar Cells*, vol. 93, no. 11, pp. 1994–2002, Nov. 2009.
[16] N. Sun *et al.*, "Bulk heterojunction solar cells with NiO hole transporting layer based on AZO anode," *Solar Energy Mater. Solar Cells*, vol. 94, no. 12, pp. 2328–2331, Dec. 2010.
[17] Y. H. Kim *et al.*, "Highly conductive PEDOT:PSS electrode with optimized solvent and thermal post-treatment for ITO-free organic solar cells," *Adv. Funct. Mater.*, vol. 21, no. 6, pp. 1076–1081, Mar. 2011.
[18] S. Choi, W. J. Potscavage, Jr., and B. Kippelen, "ITO-free large-area organic solar cells," *Opt. Exp.*, vol. 18, no. S3, pp. A458–A466, Sep. 2010.
[19] F. Guo *et al.*, "ITO-free and fully solution-processed semitransparent organic solar cells with high fill factors," *Adv. Energy Mater.*, vol. 3, no. 8, pp. 1062–1067, Aug. 2013.
[20] J. Van De Lagemaat *et al.*, "Organic solar cells with carbon nanotubes replacing InO:Sn as the transparent electrode," *Appl. Phys. Lett.*, vol. 88, no. 23, 2006, Art. ID. 233503.
[21] L. Cattin, J. C. Bernede, and M. Morsli, "Toward indium-free optoelectronic devices: Dielectric/metal/dielectric alternative transparent conductive electrode in organic photovoltaic cells," *Phys. Status Solidi A*, vol. 210, no. 6, pp. 1047–1061, Jun. 2013.
[22] W. Cao *et al.*, "Flexible organic solar cells using an oxide/metal/oxide trilayer as transparent electrode," *Org. Electron.*, vol. 13, no. 11, pp. 2221–2228, Nov. 2012.
[23] S. D. Yambem *et al.*, "Optimization of organic solar cells with thin film Au as anode," *Sol. Energy Mater. Sol. Cells*, vol. 95, no. 8, pp. 2424–2430, Aug. 2011.
[24] S. Lim, D. Han, H. Kim, S. Lee, and S. Yoo, "Cu-based multilayer transparent electrodes: A low-cost alternative to ITO electrodes in organic solar cells," *Sol. Energy Mater. Sol. C.*, vol. 101, pp. 170–175, Jun. 2012.
[25] D. Ghosh, R. Betancur, T. Chen, V. Pruneri, and J. Martorell, "Semi-transparent metal electrode of Cu–Ni as a replacement of an ITO in organic photovoltaic cells," *Sol. Energy Mater. Sol. C.*, vol. 95, no. 4, pp. 1228–1231, Apr. 2011.
[26] Z. Wang *et al.*, "Improvement of transparent silver thin film anodes for organic solar cells with a decreased percolation threshold of silver," *Sol. Energy Mater. Sol. C.*, vol. 127, pp. 193–200, Aug. 2014.
[27] Z. Wang *et al.*, "ITO-free semitransparent organic solar cells based on silver thin film electrodes," *Int. J. Photoenergy*, vol. 2014, 2014, Art. ID. 209206.
[28] R. S. Sennett and G. D. Scott, "The structure of evaporated metal films and their optical properties," *J. Opt. Soc. Amer.*, vol. 40, no. 4, pp. 203–210, Apr. 1950.
[29] S. E. Roark and K. L. Rowlen, "Thin silver films: Influence of substrate and postdeposition treatment on morphology and optical properties," *Anal. Chem.*, vol. 66, no. 2, pp. 261–270, Jan. 1994.

[30] V. Zaporojtchenko, K. Behnke, A. Thran, T. Strunskus, and F. Faupel, "Condensation coefficients and initial stages of growth for noble metals deposited onto chemically different polymer surfaces," *Appl. Surf.,Sci.*, vol. 144, pp. 355–359, Apr. 1999.
[31] G. Rosenfeld, R. Servaty, C. Teichert, B. Poelsema, and G. Comsa, "Layer-by-layer growth of Ag on Ag (111) induced by enhanced nucleation: A model study for surfactant-mediated growth," *Phys. Rev. Lett.*, vol. 71, pp. 895–898, Aug. 1993.
[32] T. R. Andersen *et al.*, "Scalable, ambient atmosphere roll-to-roll manufacture of encapsulated large area, flexible organic tandem solar cell modules," *Energy Environ. Sci.*, vol. 7, no. 9, pp. 2925–2933, May 2014.
[33] F. C. Krebs, N. Espinosa, M. Hösel, R. R. Søndergaard, and M. Jørgensen, "25th anniversary article: Rise to power - OPV-based solar parks," *Adv. Mater.*, vol. 26, no. 1, pp. 29–39, Jan. 2014.
[34] M. Hösel, R. R. Søndergaard, M. Jørgensen, and F. C. Krebs, "Fast inline roll-to-roll printing for indium-tin-oxide-free polymer solar cells using automatic registration," *Energy Technol.*, vol. 1, no. 1, pp. 102–107, Jan. 2013.